Chemical Engineering Journal 143 (2008) 180–185

Contents lists available at ScienceDirect

Chemical Engineering Journal

journal homepage: www.elsevier.com/locate/cej

Dehydroisomerization of *n*-butane over Cr/SiO_2

Gulin Selda Pozan[a,*], Aydın Tavman[b], Ismail Boz[a]

[a] *Istanbul University, Faculty of Engineering, Chemical Engineering Department, Avcilar, 34320 Istanbul, Turkey*
[b] *Istanbul University, Faculty of Engineering, Chemistry Department, Avcilar, 34320 Istanbul, Turkey*

ARTICLE INFO

Article history:
Received 31 August 2007
Received in revised form 21 March 2008
Accepted 10 April 2008

Keywords:
Cr
SiO_2
Dehydroisomerization
n-Butane
Catalyst characterization

ABSTRACT

The catalytic activity and selectivity of CrO_x/SiO_2 for the dehydroisomerization of *n*-butane were studied at 550 °C and 1 atm. Influence of chromia concentration and chromia precursor on the oxidation state, activity and selectivity were investigated. The catalysts were characterized by X-ray diffraction (XRD), TGA and temperatures programmed reduction (TPR). The isomerization activity linearly increased with increasing acidity and Cr loading. The addition of chromium precursors in complex form decreased the initial activity in dehydroisomerization of *n*-butane and but increased the selectivity of butenes. Catalyst, which had the highest acidity and lowest crystallite size, was the most active in isomerization reaction. The highest selectivity and yield of butenes achieved was 92% and 5.5%, respectively.

© 2008 Elsevier B.V. All rights reserved.

1. Introduction

The dehydroisomerization of *n*-butane to isobutene is a challenging reaction. Bifunctional catalytic activities for dehydrogenation and isomerization as well as stability toward deactivation are required.

Isobutene is a valuable intermediate used in various chemical reactions, for example, as a monomer in polymerization and copolymerization reactions, as alkylation agent in the production of methyl-tert-butyl-ether (MTBE) and in the production of isoprene. Isobutane is a starting material for producing isobutene (2-methyl-propene) by a dehydrogenation process. Isobutene can be reacted with methanol or ethanol to produce MTBE or ethyl-tert-butyl-ether (ETBE). Both are useful as gasoline additives because they have good antiknocking properties. MTBE, alkylate and light isoparaffins are alternative octane enhancers with fewer environmental objections. In the refining industry, the main processes for producing branched alkanes are the skeletal isomerization of linear saturated hydrocarbons.

Pt-promoted [1–3] chlorided alumina, a widely used alkane isomerization catalyst, has also raised environmental concern for many years, because it requires chlorine treatment during operation to avoid activity loss. Zeolite catalysts are also already used in aromatization processes [4–6] and could be used in isobutane–butene alkylation. Supported chromium oxides are industrially important group of catalytic materials. They are used in oxidation, polymerization, dehydrogenation/hydrogenation [7]. However, the Cr^{6+} oxidant is usually not regenerated and the toxic effluents result in serious drawbacks, especially on an industrial scale. In order to partially overcome this problem, the use of chromium reagents adsorbed on inert supports has been utilised.

The goal of this research is to compare a series of Cr/SiO_2 catalyst by correlating the synthesis conditions, impregnation and ligand containing precursors with *n*-butane dehydrogenation/isomerization activities.

2. Experimental

2.1. The preparation of catalyst of Cr^{3+}/SiO_2 (SCr_x)

The catalyst support was SiO_2 from Fluka with a surface area of 320 m^2/g (35–75 mesh ASTM) determined after calcination at 570 °C for 18 h. CrO_x/SiO_2 catalysts were prepared by incipient wetness impregnation from aqueous solution of $Cr(NO_3)_3{\cdot}9H_2O$ (>97%, Fluka). The wet samples were stored overnight at room temperature, dried at 60 °C for 16 h under vacuum, and treated in flowing nitrogen at 570 °C for 13 h. Cr loading of the catalysts was 1, 6 and 11 wt%. The catalysts are labeled as SCr_x and suffix S represents standard preparation involving no chromia complexes as precursors and involves SiO_2 as support and *x* represents chromia loading as weight percentages. Same silica support is used in all preparation.

---

* Corresponding author. Tel.: +90 212 473 70 70x17665; fax: +90 212 473 71 80.
E-mail addresses: gpozan@istanbul.edu.tr (G.S. Pozan), ismailb@istanbul.edu.tr (I. Boz).

1385-8947/$ – see front matter © 2008 Elsevier B.V. All rights reserved.
doi:10.1016/j.cej.2008.04.004

Table 1
BET surface areas, Cr^{6+} and Cr^{3+} contents of catalysts, Cr_2O_3 crystallite sizes and Cr_2O_3 phase crystallinity, conversions and selectivities of butenes after 20 min of time-on-stream

Catalysts	Surface areas (m^2/g)	% Cr^{6+} (w/w)	% Cr^{3+} (w/w) ($Cr_{total}-Cr^{6+}$)	Cr_2O_3 Crystallite size (nm)–Cr_2O_3 Crystallinity (%)	Selectivity % (Butenes)	Conversion of *n*-butane (%)
SCr_{11}	363	1.90	8.6	16.1–74	85.1	6.8
SCr_6	375	1.74	3.66	7.1–41	5.2	18.2
SCr_1	371	0.64	0.21	4.2–23	3.9	23.6
$SLCr_{11}{}^{3+}$	385	1.71	8.59	17.2–78	87.2	4.8
$SLCr_6{}^{3+}$	395	1.50	4.2	10.6–48	5.3	13.7
$SLCr_1{}^{3+}$	376	0.45	0.46	4.3–23	4.5	24.9
$SLCr_{11}{}^{3+/6+}$	386	0.65	8.48	21.3–81	92.0	3.9
$SLCr_6{}^{3+/6+}$	375	0.30	5.2	12.5–52	6.0	18.2
$SLCr_1{}^{3+/6+}$	431	0.15	0.73	4.5–26	4.7	39.2

2.2. *The preparation of catalyst in the presence of fenil benzimidazol (FB) ligand ($SLCr_x{}^{3+/6+}$)*

233 mg (1.2 mmol) FB ligand was dissolved in 20 ml ethanol. 78 mg K_2CrO_4 was added into the solution. 160 mg (0.4 mmol) $Cr(NO_3)_3{\cdot}9H_2O$ was also added to this mixture. The solution was heated up to 40 °C and stirred for 2 h and formed precipitate was filtered and dried at room temperature. A dark brown component was formed. Later, the crystals in the precipitate was filtered and dried. A light brown structure was formed. 12 mg Cr–FB complex was dissolved in ethanol as 11%, 6%, and 1% Cr (w/w) would exist in the catalyst and the solution was added to 35–75 mesh SiO_2. The obtained paste was left for drying overnight. Then, it was dried under 10 mm Hg vacuum at 60 °C for 16 h. Finally, the dired sample was placed into alumina crucibles and then heated under nitrogen at 570 °C for 13 h. In this preparation route, FB ligand can create complexes with both Cr^{3+} and Cr^{6+}, they are labeled as $SLCr_x{}^{3+/6+}$. L represents that ligand was utilised as precursor and *x* represents Cr content as weight percentages. Since FB ligand can make complexes both with Cr^{3+} and Cr^{6+}, L suffix and oxidation levels were kept in acronyms. For instance, $SLCr_x{}^{3+/6+}$ means *x*% chromia supported on SiO_2 and prepared with ligand which contained Cr^{3+} and Cr^{6+}.

2.3. *The preparation of catalyst in the presence of methyl hydroxy fenil benzimidazol (MHFB) ligand ($SLCr_x{}^{3+}$)*

224 mg (1 mmol) MHFB ligand was dissolved in 30 ml ethanol. 215 mg (0.5 mmol) $Cr(NO_3)_3{\cdot}9H_2O$ was added into the solution. The solution was heated up to 40 °C and stirred for 2 h and precipitate was filtered and dried at room temperature. A dark brown component was formed. Later, the crystals in the precipitate was filtered and dried. A dark green structure was formed. 23 mg Cr–MHFB complex was dissolved in ethanol as 11%, 6%, 1% Cr (w/w) would exist in catalyst compound and the solution was added to 35–75 mesh SiO_2. The obtained paste was left for drying overnight. Later, it was dried under vacuum at 60 °C for 16 h. Finally, the dired sample was placed into ceramic crucibles and then heated under nitrogen at 570 °C for 13 h. They are labeled as $SLCr_x{}^{3+}$, and *x* represents Cr content as weight percentages.

2.4. *Catalyst characterization*

Surface areas of the catalysts after calcining under nitrogen at 570 °C for 13 h is measured by a Costech sorptometer 1042 equipment. Results are obtained after drying the samples in situ at 250 °C for 2 h and tabulated in Table 1.

Chromia speciation was first achieved by spectroscopic method. Cr^{6+} in the samples was determined by a colorimetric procedure, namely, diphenylcarbazide (DPC) spectrophotometry [8,9]. The sample was heated in a muffle furnace for 1 h at 560 °C, Cr^{6+} was dissolved as $CrO_4{}^{2-}$ from the samples in 0.5 M H_2SO_4 in deionized water. In this method, Cr^{5+}, if present in the sample, may be dissolved together with Cr^{6+} [10]. The amount of Cr^{5+} in the supported catalysts was assumed to be very small [10,11]. 0.05 M solution of the Cr^{6+} reagent, diphenylcarbazide, was prepared by dissolving 0.6056 g in 50 ml of acetone. The solutions were prepared by dissolving the appropriate amount of samples in 0.5 M H_2SO_4 and DPC in distilled water. This solution was used as a calibration mixture. The concentration of Cr^{6+} was measured using a Carry 1 E UV–vis spectrophotometer at 540 nm.

The total amount of chromia available was measured using a Varian Spectra Fast Sequential −220 atomic absorption spectrometer with an air-acetylene flame. The total chromium content is calculated as the sum of Cr^{3+} and Cr^{6+}. Cr^{3+} that existed on the surface was calculated by difference.

The crystal phases were determined by X-ray diffraction (XRD), from Rigaku D/Max-2200 diffractometer by using Cu Kα ($\lambda = 1.5405$) radiation. Samples were scanned from 10 to 60 at a rate of 0.5°/min (in 2Θ). The sizes of the crystalline domains (Cr_2O_3) were obtained via the Scherer equation ($t = C\lambda/B\cos\Theta$) where λ is the X-ray wavelength (A°), *B* is the full width at half maximum, Θ is Bragg angle, *C* is a factor depending on crystallite shape (taken to be one), and *t* is the crystallite size (A°).

TPR profiles were obtained by using Quantachrome ChemBET 3000 flow type equipment. In TPR experiments, 60 mg of the catalyst was dried at 105 °C for 2 h, and 10% H_2/N_2 was used as a reducing gas. Temperature ramp rate was 10 °C/min and flow rate was 70 ml/min. The effluent was passed through liquid N_2 trap to remove water and CO_2. The changes in H_2 flow were followed using a thermal conductivity detector.

2.5. *Catalyst testing*

Cr/SiO_2 catalysts were examined for their selectivity and activity in *n*-butane dehydroisomerization. For this purpose, 0.5 g of sample was mixed with 5 g of quartz of the same size and placed into a quartz reactor of 4 mm inner diameter. The conversions of butane over various catalysts were measured at 550 °C, at atmospheric pressure and with a weight hourly space velocity (WHSV) of 7 h^{-1} in three different modes:

(1) *n*-Butane (4 ml/min) was diluted with nitrogen, the molar ratio of nitrogen to *n*-butane being 8:1. Prior to experiment, the catalyst was reduced at 550 °C with 20% hydrogen (8 ml/min) for 30 min.
(2) Prior to the reaction, the catalyst was not reduced with hydrogen. A reactant stream (n-$C_4/H_2 = 1/2$) containing *n*-butane + 20% H_2 in a balance of N_2.

(3) Some experiments were run using *n*-butane diluted with nitrogen without any prior reduction.

The reactor effluent was analyzed by an on-line gas chromatograph fitted with Al_2O_3 column. After 10 min, the reactor effluent was analyzed by direct injection into GC and then at intervals of 30 min (e.g., 40, 70, 100).

The conversion and selectivity were calculated from the reaction product on the basis of the carbon balance: the total molar amount of carbon in the effluent was assumed to be equal to the molar amount of carbon in the *n*-butane fed to the reactor. The coke formed on the catalyst during the dehydroisomerization test was neglected. The total amount of *n*-butane fed to the reactor equals $C_{nb_{in}}$.

$$C_{nb_{in}} = \Sigma C_1 \times \frac{1}{4} + \Sigma C_2 \times \frac{2}{4} + \Sigma C_3 \times \frac{3}{4} + \Sigma C_4 + C_6 \times \frac{6}{4} + C_7 \times \frac{7}{4}, \tag{1}$$

where C_i = molar amount of product containing *i* carbon in the reactor effluent, including hydrocarbons, CO, and CO_2. The conversion of *n*-butane equals X_{nb}.

$$X_{nb} = 100 \times \frac{C_{nb_{in}} - C_{nb_{out}}}{C_{nb_{in}}} \tag{2}$$

where $C_{nb_{in}}$ = the amount of *n*-butane fed to the reactor calculated according to Eq. (1) and $C_{nb_{out}}$ = the amount of *n*-butane in the reactor effluent. The selectivity to a specific product, for example, *n*-butenes, S_{nb} was calculated as

$$S_{nb} = 100 \times \frac{C_{nb}}{C_{nb_{in}} - C_{nb_{out}}} \tag{3}$$

where C_{nb} = amount of *n*-butenes, 1-butene, cis-2-butene, and trans-2-butene in the reactor effluent.

The yield of a specific product was obtained by multiplying the *n*-butane conversion by the corresponding selectivity. Experimental repeatability was around ±14%. This was calculated from four repeated experiments done at a representative reaction condition with fresh catalysts of the same type and used as a measure of repeatability.

3. Results and discussion

3.1. X-ray powder diffraction

The diffraction patterns of various catalysts are shown in Figs. 1 and 2, respectively. Concerning the SCr catalysts, XRD patterns match the diffraction pattern of Rhombohedral α-Cr_2O_3. α-Cr_2O_3 crystals should give a characteristic X-ray diffractogram with well-defined most intensive peaks corresponding to the planes with *h k l* (1 0 4), (1 1 0), (1 1 6), (0 1 2), (0 2 4) and (3 0 0) [12]. The superposition of (0 1 2), (1 0 4) and (1 1 0) peaks of Cr_2O_3 phase with 75, 100 and 95% relative intensities and amorphous halo of silica did not allow to use these peaks for calculation of chromia concentrations. For the samples, segregation of α-Cr_2O_3 is apparent on the 11% Cr loaded sample, whereas for 6% Cr and 3% Cr loaded SCr samples α-Cr_2O_3 segregation is not well observed.

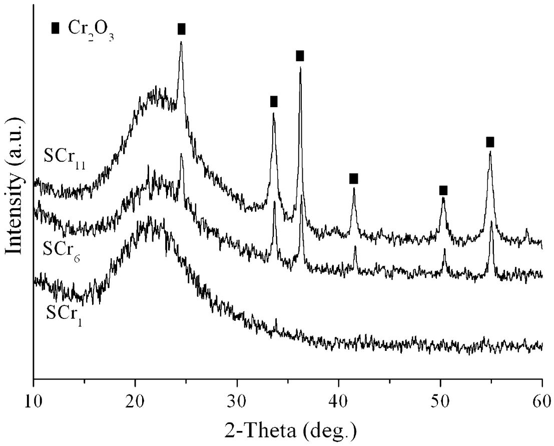

Fig. 1. The diffraction patterns of SCr_x catalysts.

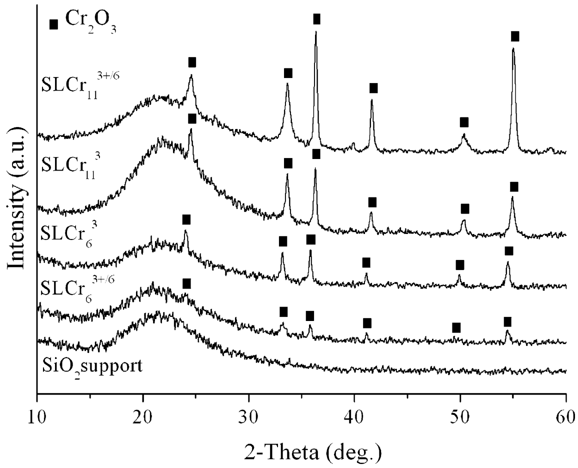

Fig. 2. The diffraction patterns of $SLCr_x^{3+}/^{6+}$ and $SLCr_x^{3+}$ catalysts.

From XRD patterns, it was noticed that the addition of chromium in the form of FB and MHFB complexes shifted the position of Cr_2O_3 phase and changed the available phases in the catalysts. 2θ signals of Cr_2O_3 shifted to higher values. It also affected the relative intensities of (1 0 4) and (1 1 0) peaks. The quantities of crystalline Cr_2O_3 phase in catalysts were calculated from the relative integral intensities of XRD peak corresponding to (1 1 6) plane (81% relative intensity) that was not affected by silica. Based on these differences % crystallinity of Cr_2O_3 phase in samples were calculated and listed in Table 1. Crystallinity of Cr_2O_3 was much higher in catalyst SCr_{11}^{3+} (81%) compared with catalyst SCr_6^{3+} (52%), while the lowest crystallinity (26%) was detected in catalyst SCr_1^{3+}. Crystallinities followed a similar trend for the other two catalysts prepared with ligands. Highest crystallinity values were obtained at the highest chromium loadings.

3.2. Temperature programmed reduction

The TPR profiles of the catalysts as a function of temperature are shown in Figs. 3 and 4. Two peaks at 278 °C and 435 °C were detected over the SCr_{11} catalyst. In case of chromia supported on SiO_2 at low metal loading, 6% and 1%, most of H_2 was consumed at high temperature region (peaks at 435 °C). Increasing the chromia loading to 11 wt.% yielded a substantial change of TPR spectra so that most of the hydrogen was consumed at lower temperature (peak centered at 278 °C) [13]. Reducibility of the catalysts was facilitated as the chromium loading increased.

For the catalysts prepared with ligand containing precursors, TPR spectra recorded maximums at 335 °C and at 445 °C. For $SLCr_{11}^{3+/6+}$ catalyst maximum was at 335 °C and 445 °C and for $SLCr_{11}^{3+}$ catalyst, observed maximum was at 335 °C. The utilization of ligand in precursor caused an increase in reduction temperatures compared to noligand containing catalysts. With increasing Cr loading, H_2 consumption relative to the amount of Cr^{6+} decreased, indicating formation of Cr^{3+}. The extent of the reduction of Cr^{6+} in

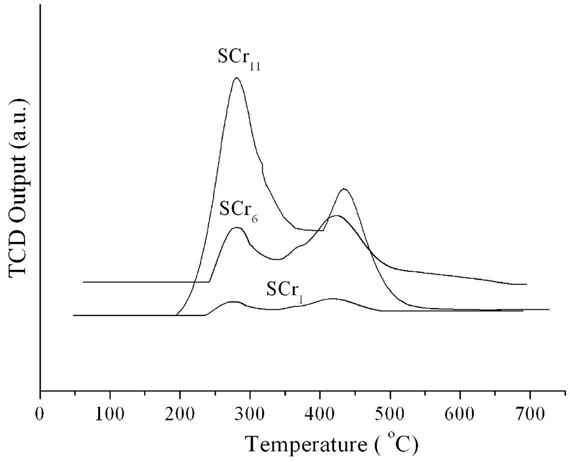

Fig. 3. TPR profiles of various SCr_x^{3+} catalysts.

the catalysts was calculated from the H_2 consumption by assuming that (i) H_2 was consumed only in the reduction of Cr^{6+} species, (ii) reduction yielded Cr^{3+} species. Since under typical reaction conditions the catalysts all are in their reduced state, it is obvious that conversion and selectivities were to be found not very much varying under circumstances. However, depending on the reduction temperatures, surface availability and sintering behavior of reduced species will change accordingly.

3.3. Acidity measurements

Amine adsorption method on acid sites of solid catalysts is a well-known technique to determine the acidity of the catalyst. The use of *n*-butylamine as molecular probe for the characterization of catalysts has been reported [14–16]. Derivative thermogravimetry (DTG) desorption curves of *n*-butylamine are shown in Fig. 5. As shown in Fig. 5, catalysts have three desorption steps depending on their acidity. These are the desorption of physysorbed *n*-butylamine before 117 °C, dissociation of *n*-butylamine from medium acid sites of the catalysts indicated by the second peak in DTG curves at about 300 °C, and dissociation of the *n*-butylamine from strong acid sites of the catalysts indicated by the third peaks in the curves at 483–979 °C.

SCr_{11} has the highest peak intensity in medium acid sites. SCr_{11}, $SLCr_{11}^{3+/6+}$, and $SLCr_{11}^{3+}$ have both medium and strong acidity compared to the chromium containing catalysts with low amounts (e.g., 6% and 1%). Based on weight loss values of *n*-butylamine treated catalysts, amount of adsorbed *n*-butylamine was calculated quantitatively. As shown in Fig. 6, acidity was found to decrease in following order: $SCr_{11} > SLCr_{11}^{3+} > SLCr_{11}^{3+/6+}$. Weak acidity obtained from ligand containing precursors was thought to be due to residues left on the acidic sites. Residues emanate from high temperature calcination and reduction of ligands.

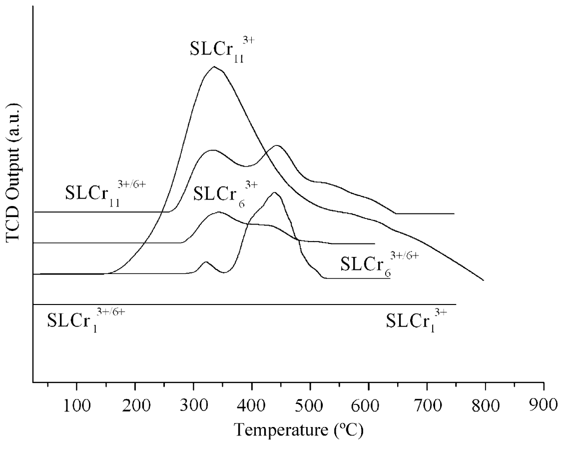

Fig. 4. TPR profiles of various $SLCr_x^{3+}$ and $SLCr_x^{3+}/^{6+}$ catalysts.

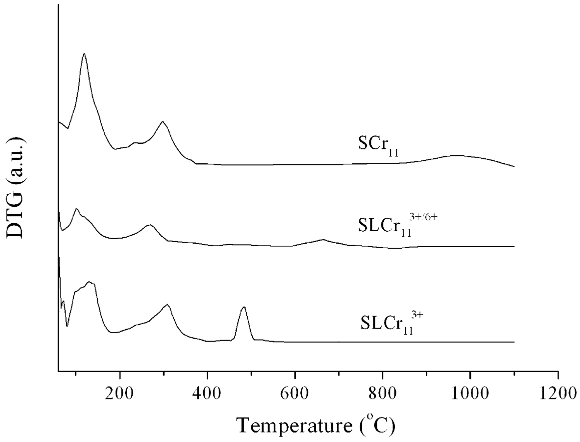

Fig. 5. DTG desorption curves of *n*-butylamine for various catalysts.

3.4. Conversion of n-butane

The *n*-butane conversion increased with increasing Cr content up to 11%, above which all values remained relatively constant. Therefore, discussions were restricted to the loadings 11% as upper limit of loading. The isobutene selectivity was constant at approximately 80% regardless of Cr content. Cr 11 wt.% improved isobutene selectivity and stability of catalytic activity with time. Fig. 7a–c shows the effect of addition of hydrogen, prior reduction and without reduction with respect to time-on-stream over the catalysts prepared without any ligand in precursor.

Isobutene selectivity improved as the Cr^{3+}content increased in all catalysts. The conversions in isomerization reactions declined strongly over the first 40 min of reaction. The addition of both ligands to precursors caused an increase in butenes selectivity compared to SCr_{11} catalysts. Butenes selectivity decreased in the following order: $SLCr_{11}^{3+/6+} > SLCr_{11}^{3+} > SCr_{11}$. On the other hand, butenes selectivity increased with increasing Cr loading as listed in Table 1.

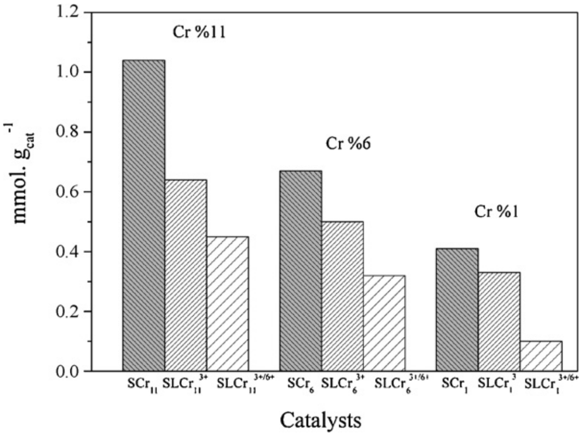

Fig. 6. Amount of *n*-butylamine adsorbed over various catalysts.

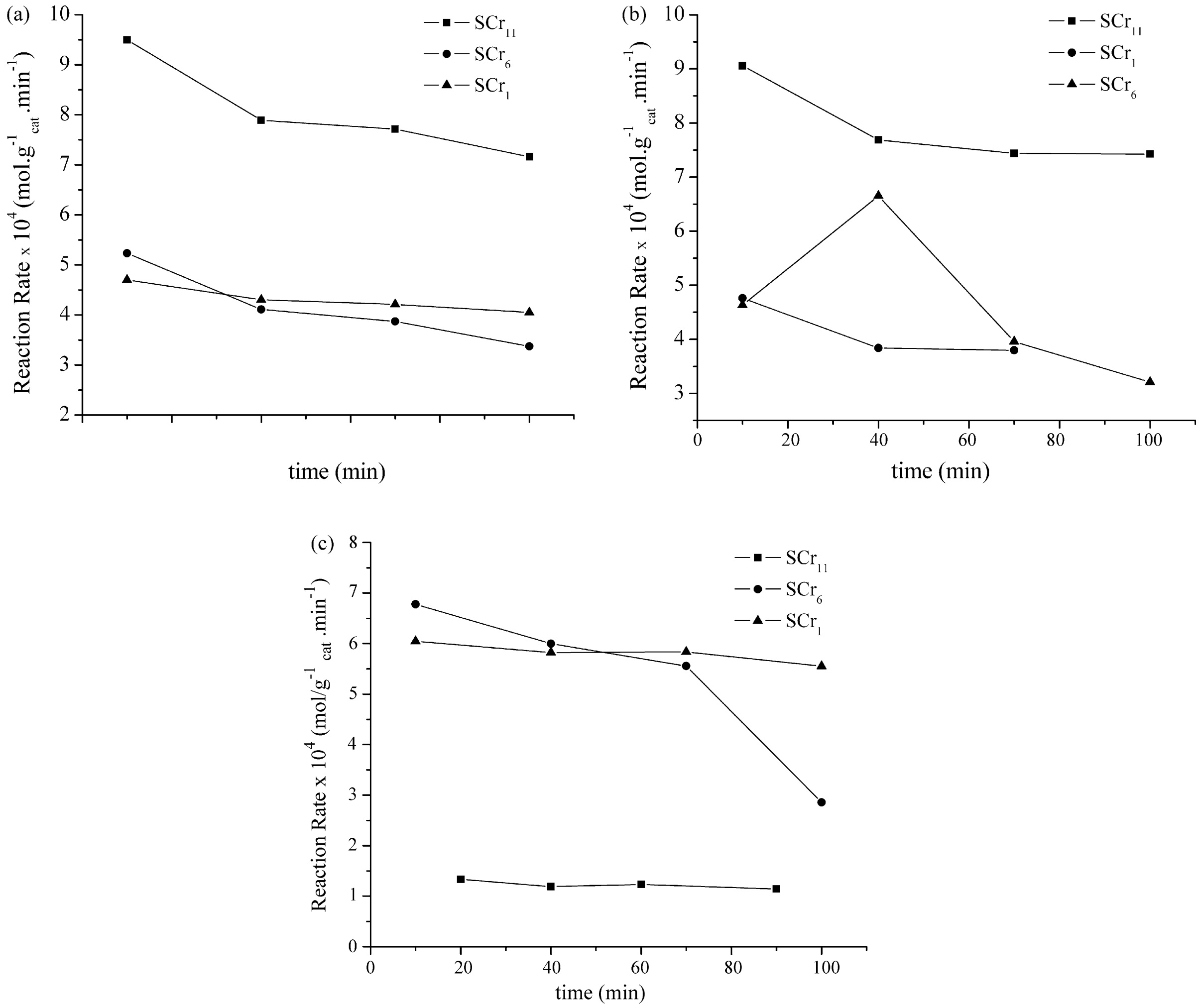

Fig. 7. (a) Changes in reaction rate of *n*-butane at various Cr loading (H_2+*n*-butane, 2:1).
(b) Changes in reaction rate after reduction.
(c) Changes in reaction rate without reduction.

High initial reaction rate was obtained over butane + H_2 (4 ml/min *n*-butane + 8 ml/min H_2) over SCr_{11} catalyst. In Fig. 7b, at 550 °C, the catalysts were tested after being reduced for 30 min. Initial reaction rates were found to decrease. However, *n*-butane and N_2 present in reactant stream, at 550 °C, reactivity decreased too.

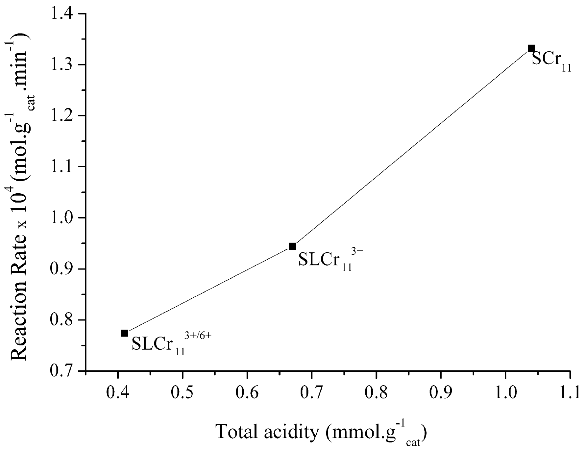

Fig. 8. The variation of initial reaction rate with respect to total acidity.

Fig. 8 shows the correlation between total acidity and the initial reaction rate. A good correlation between total acidity and the initial reaction rate was found for the SCr_{11} catalysts. Initial reaction rate and selectivity obtained at the same representative reaction conditions for all catalysts were listed in Table 1. There is a general consensus in the literature that the activity pattern of Cr-based dehydrogenation catalysts depended on the overall Cr loading, the dehydrogenation temperature and the time-on-stream [17]. The initial dehydrogenation activity increased, linearly with increasing Cr loading. However, at Cr loading typically higher than 11 wt% Cr, the activity gain leveled off [18]. Furthermore, the overall activity decreased with increasing time-on-stream. The same decreasing trends in activity were found for all Cr^{6+} and Cr^{3+} containing catalysts. However, with the present knowledge, it is almost impossible to discriminate between the individual contributions of these Cr^{3+}-centers to the overall catalytic conversion and selectivity. Nevertheless, there are indications that surface Cr^{6+}-ions, forming the dispersed surface phase on the silica and/or chromia (Cr_2O_3), were precursors for the Cr^{3+}-induced isomerization/dehydroisomerization. Hakuli et al. [19] have demonstrated that the initial dehydrogenation activity was directly proportional to the initial amount of surface Cr^{6+}.

As the Cr percentage increased, the crystal size of Cr_2O_3 and the crystallinity of Cr_2O_3 phase increased. The use of complex caused an increase in the crystal size. The increase in crystal size and cystallinity occurred parallel with an increase in selectivity of butenes.

At all Cr loadings, both Cr^{6+} and Cr^{3+} were detected, the amount of Cr^{6+} decreased as Cr oxide loading increased. In addition, from literature, it was found the polychromate/chromate ratio increased with increasing Cr loading, indicating that less (reactive) hydroxyl groups were available to stabilize the surface chromium oxide as an anchored chromate species [20]. At all Cr loadings, Cr^{3+} was the dominant species and the fraction of Cr^{6+} was comparatively low. The latter can be present as either crystalline α-Cr_2O_3, which is XRD-detectable, and amorphous Cr_2O_3. The negligible conversions obtained with low Cr loadings were attributed to the stabilization in or on support rendering them catalytically inactive. This type of stabilization effect is more apparent over Al_2O_3. Zeolite supports of various SiO_2/Al_2O_3 ratios, e.g., ZSM5, is typically good catalysts for the dehyroisomerisation of *n*-butane. Its shortcoming is high selectivity to by-products at high conversions emanating from oligomerisation/cracking of butenes on the acid sites. Supports of all types must have a low activity for the prolytic cracking of *n*-butene [21].

4. Conclusions

The catalytic performance of various Cr/SiO_2 catalyst at 550 °C for dehydrogenation/isomerization of *n*-butane was examined. Addition of 11% Cr unquestionably improved the isobutene selectivity. The isomerization activity almost linearly increased with increasing Cr loading. Complex addition of Cr decreased the initial reaction rate of dehydroisomerization of *n*-butane and but increased selectivity to butenes. At 550 °C and after reduction for 30 min before reaction, initial reaction rate decreased. The addition of ligand caused an increase in Butenes selectivity. Isomerization activity of silica supported catalysts were in the order of $SCr_{11} > SLCr_{11}{}^{3+} > SLCr_{11}{}^{3+/6+}$. SCr_{11} catalyst, which had the highest acidity and highest crystallite size, was the most active in isomerization reaction. The best selectivity to butenes, 92%, was obtained with the $SLCr_{11}{}^{3+/6+}$ catalyst. The highest yield of *n*-butenes achieved, 5.5%, was from SCr_{11} catalyst.

Acknowledgement

This work was supported by the Research Fund of The University of Istanbul.

References

[1] B.Q. Xu, W.M.H. Sachtler, J. Catal. 167 (1997) 224–233.
[2] R.A. Srinivasan, R.A. Keogh, D.N. Milburn, B.H. Davis, J. Catal. 153 (1995) 123–130.
[3] K. Föttinger, K. Zorn, H. Vinek, Appl. Catal. A: Gen. 284 (2005) 69–75.
[4] G. Caeiro, R.H. Carvalho, X. Wang, M.A.N.D.A. Lemos, F. Lemos, M. Guisnet, F. Ramôa Ribeiro, J. Mol. Catal. A: Chem. 255 (2006) 131–158.
[5] X. Li, E. Iglesia, J. Catal. 255 (2008) 134–137.
[6] H.J. Jung, S.S. Park, C.-H. Shin, Y.-K. Park, S.B. Hong, J. Catal. 245 (2007) 65–74.
[7] Z. Chajar, M. Primet, H. Praliaud, M. Chevrier, C. Gauthier, F. Mathis, Appl. Catal. B 4 (1994) 199–211.
[8] M. Llobat-Estelles, A.R. Mauri-Aucejo, M.D. Lopez-Catalan, Fresenius J. Anal., Chem. 371 (2001) 358.
[9] S. Yalcin, R. Apak, Anal. Chim. Acta 505 (2004) 25–35.
[10] S. DeRossi, M.P. Casaletto, G. Ferraris, A. Cimino, G. Mineli, Appl. Catal. 167 (1998) 257–270.
[11] B.M. Weckhuysen, L.M. De Ridder, P.J. Grobet, R.A. Schoonheydt, J. Phys. Chem. 99 (1995) 320–326.
[12] CPDS-ICDD 38 (1994) 1479.
[13] C.M. Pradier, F. Rodrigues, P. Marcus, M.V. Landau, M.L. Kaliya, A. Gutman, M. Herskowitz, Appl. Catal. B: Environ. 27 (2000) 73–85.
[14] V.J. Fernandes, A.S. Araujo, G.J.T. Fernandes, J. Therm. Anal. Calorim. 56 (1999) 275–285.
[15] D.R. Milburn, K. Saito, R.A. Keogh, B.H. Davis, Appl. Catal. A: Gen. 215 (2001) 191–197.
[16] R. Bezman, J. Catal. 68 (1981) 242–244.
[17] C.P. Poole, D.S. Maciver, Adv. Catal. 17 (1967) 223–314.
[18] B.M. Weckhutsen, R.A. Schoonheydt, Catal. Today 51 (1999) 223–232.
[19] A. Hakuli, A. Kytokivi, A.O. Krause, T. Suntola, J. Catal. 161 (1996) 393–400.
[20] B.M. Weckhuysen, R.A. Schoonheydt, J.M. Jehng, I.E. Wachs, S.J. Cho, R. Ryoo, S. Kijlstra, E. Poels, J. Chem. Soc., Faraday Trans. 91 (1995) 3245–3253.
[21] G.D. Pirngruber, K. Seshan, J.A. Lercher, J. Catal. 190 (2000) 374–386.